Atmospheric Environment 356 (2025) 121288

Contents lists available at ScienceDirect

Atmospheric Environment

journal homepage: www.elsevier.com/locate/atmosenv

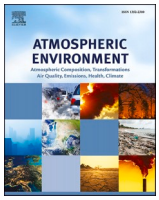

Conceptual study on spatial distribution fluctuations of $PM_{2.5}$ concentration on the Korean Peninsula in winter related to synoptic meteorological clusters

Daeun Chae [a], Jung-Woo Yoo [b], Jiseon Kim [a], Soon-Hwan Lee [b,c,*]

[a] Department of Earth Science, Pusan National University, Busan, 46241, Republic of Korea
[b] Institute of Environmental Studies, Pusan National University, Busan, 46241, Republic of Korea
[c] Department of Earth Science Education, Pusan National University, Busan, 46241, Republic of Korea

HIGHLIGHTS

- Identified synoptic patterns are associated with $PM_{2.5}$ on the Korean Peninsula.
- Different $PM_{2.5}$ distributions appear in similar synoptic systems.
- The difference in $PM_{2.5}$ distribution is due to small differences in the synoptic system.
- Location and intensity of high/low pressure systems played an important role in $PM_{2.5}$.

ARTICLE INFO

Keywords:
Synoptic patterns
K-means clustering analysis
$PM_{2.5}$ pollution standards
Korean Peninsula

ABSTRACT

To classify prevailing synoptic patterns on the Korean Peninsula during the seasonal $PM_{2.5}$ management from 2015 to 2019, K-means clustering analysis was performed using 925 hPa geopotential height from the National Centers for Environmental Prediction (NCEP) Final Analysis (FNL) data. Additionally, we analyzed synoptic patterns based on the $PM_{2.5}$ pollution standards for each cluster to understand the differences in high and low $PM_{2.5}$ concentrations under similar synoptic meteorological conditions. The synoptic patterns were classified into five types. Clusters (C1, C3, C4) with a west-high, east-low pressure distribution experienced worsened $PM_{2.5}$ levels due to a reduction in the east-west pressure gradient. This weakening caused the northwesterly winds to slow down, leading to the accumulation of pollutants. Clusters (C2, C5) with a south-high, north-low pressure pattern were characterized by conditions of high $PM_{2.5}$, when a high-pressure system over the southeastern region of the Korean Peninsula approached or receded from the Korean Peninsula, accompanied by a reduction in the pressure gradient. This study confirms that the intensity and location of high pressure can lead to variations in air quality under similar synoptic meteorological conditions.

1. Introduction

Aerosol pollution has become a major environmental concern as particle pollutant concentrations on the Korean Peninsula have increased over the past decade owing to rapid urbanization, population growth, and industrial and economic growth (Eck et al., 2020; Ku et al., 2021). In particular, high concentrations of $PM_{2.5}$, with a diameter less than or equal to 2.5 μm, have significant adverse effects on human health, socioeconomics, and the environment (Han et al., 2023; Lee et al., 2022; Liu et al., 2020). The causes of $PM_{2.5}$ pollution include high anthropogenic emissions, regional transport of pollutants, unfavorable meteorological conditions, and the formation of secondary aerosols. However, these factors are largely controlled by large-scale synoptic meteorological events, which can affect the formation, deposition, and transport of air pollutants (Mao et al., 2020; Miao et al., 2017). In addition, while the emission sources are more closely related to long-term $PM_{2.5}$ concentration trends and variability, meteorological conditions such as atmospheric circulation significantly influence short-term $PM_{2.5}$, such as daily, seasonal, and annual variability (Jeong et al., 2023; Lu et al., 2021).

* Corresponding author. Department of Earth Science Education, Pusan National University, Busan, 46241, Republic of Korea.
E-mail address: withshlee@pusan.ac.kr (S.-H. Lee).

https://doi.org/10.1016/j.atmosenv.2025.121288
Received 2 February 2024; Received in revised form 1 May 2025; Accepted 8 May 2025
Available online 12 May 2025

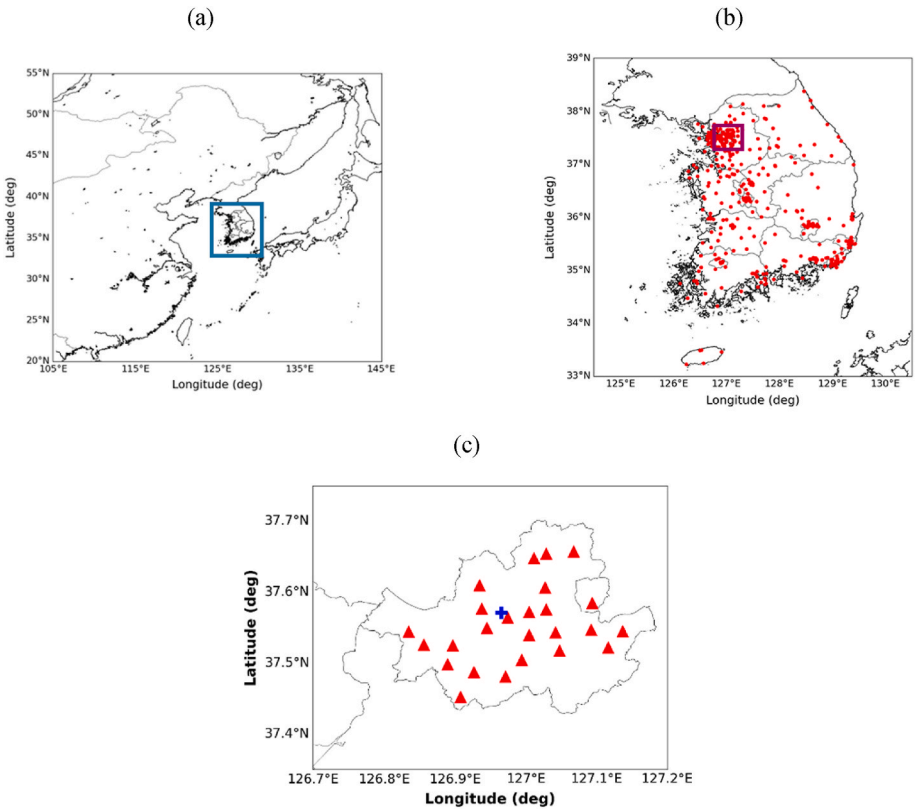

Fig. 1. (a) The domain used for synoptic patterns clustering. (b) the distribution of the Air Quality Monitoring Stations in Korean Peninsula (red circles). (c) the distribution of AQMS (red triangles) and ASOS (blue cross) in Seoul. (For interpretation of the references to colour in this figure legend, the reader is referred to the Web version of this article.)

Many studies have been conducted to understand the relationship between weather patterns at the synoptic scale and $PM_{2.5}$ pollution. Zhao et al. (2018) found that a weakened Siberian high led to decreased northwesterly winds, which contributed to the increase in $PM_{2.5}$ pollution days in the North China Plain (NCP). Gong et al. (2022) analyzed relationship between the clustered six synoptic patterns and the pollutant concentrations for three regions in China. It found that the synoptic patterns affect $PM_{2.5}$ and O_3 concentrations and are characterized differently in each region. Lee et al. (2022) classified synoptic weather patterns using the Spatial Synoptic Classification (SSC) method and found that weather patterns with warm and dry conditions contribute to high $PM_{2.5}$ concentrations in spring and winter on the Korean Peninsula, while cold and wind weather patterns have a significant impact on low $PM_{2.5}$ concentrations. Hsu and Cheng (2016) used K-means clustering analysis to classify synoptic patterns to characterize high $PM_{2.5}$ concentrations in Yunlin County, Taiwan, and found that the high $PM_{2.5}$ concentration occurs when Taiwan is under the influence of weak synoptic weather conditions and continental high-pressure, and low $PM_{2.5}$ concentrations occurs under the influence of strong southwesterly monsoonal flow. Wang and Zhang (2020) identified six typical synoptic weather patterns over the BTH region during winter from 2013 to 2018. The results revealed that a high $PM_{2.5}$ concentration in winter in the BTH region occurred when there was a weak pressure gradient or high pressure over the BTH region.

Many studies have analyzed the relationship between synoptic meteorological conditions and air quality; however, most of these studies were based on episodes of high air pollution. Studies analyzing entire days, including high and low concentrations of particulate pollutants, simply describe the characteristics of the synoptic patterns affecting high and low concentrations and do not clearly present the differences in meteorological conditions between clean and polluted days. In addition, there were both clean days and polluted days in a similar cluster when the synoptic patterns affecting $PM_{2.5}$ concentrations were classified using cluster analysis. In this study, K-means clustering analysis was performed to identify the major synoptic patterns occurring on the Korean Peninsula during the seasonal $PM_{2.5}$ management from 2015 to 2019. We analyzed the synoptic patterns and meteorological characteristics of each cluster based on $PM_{2.5}$ concentration standards in Seoul to quantitatively and qualitatively analyze the differences between high and low $PM_{2.5}$, under similar synoptic meteorological conditions.

2. Data and methods

2.1. Air quality and meteorological data

When examining the frequency of monthly occurrence on high $PM_{2.5}$ episodes and the monthly average $PM_{2.5}$ concentrations in the Korean Peninsula, high $PM_{2.5}$ episodes and average $PM_{2.5}$ concentrations was notably high during the spring and winter seasons. In this study, seasonal $PM_{2.5}$ management (January, February, March, and December) from 2015 to 2019 was selected as the study period, and Asian dust events were excluded (The total study period: 588 days). The hourly $PM_{2.5}$ concentrations were used to understand the distribution of the $PM_{2.5}$ concentration on the Korean Peninsula according to the synoptic pattern. Fig. 1b and c shows the distribution of the Air Quality Monitoring Stations in Korean Peninsula (359 stations) and Seoul (25 stations) used in this study, and the monitoring sites with observation data over five years were selected, considering the study period. The daily mean $PM_{2.5}$ concentration was calculated when more than 18 hourly data points existed a day after removing missing values. For Seoul, the average concentration from 25 stations was used.

The 925 hPa geopotential height, u and v wind components, and planetary boundary layer (PBL) height were obtained from the National

Centers for Environmental Prediction (NCEP) FNL (Final) Operational Global Analysis reanalysis with a horizontal resolution of 1° × 1°. The $PM_{2.5}$ concentration is maximum in the lower troposphere, is highly influenced by the lower atmosphere. However, friction occurs at ground level because of the complex terrain, and the influence of synoptic meteorology is significant at 850 hPa. Therefore, we selected the 925 hPa altitude, which is representative of the meteorological field in both the middle atmosphere and the surface, to exclude the friction force due to the terrain and to examine the meteorological influence on the $PM_{2.5}$ concentration within the atmospheric boundary layer. Since meteorological fields change continuously, using daily average data will not clearly reveal the differences in meteorological fields between two consecutive days. Radio sonde data is primarily provided at 0000UTC and 1200UTC. In particular, the coverage of radio sonde data is more comprehensive at 0000UTC than at other times, resulting in higher accuracy of assimilation data (Ning et al., 2019; Zhang et al., 2016). Therefore, the meteorological factors for geopotential height, u and v wind components were based on data from 0000UTC. The daily mean PBL heights (0000 UTC, 0600UTC, 1200UTC, and 1800UTC) were calculated to remove disturbances. In addition, daily average temperature, wind speed, and relative humidity data observed at 108 sites of the Automated Synoptic Observing System (ASOS) in Seoul were used to analyze the meteorological characteristics of the Seoul area.

2.2. Methods

2.2.1. Synoptic pattern classification

In this study, K-means clustering analysis was performed on the domain covering 20°N to 55°N and 105°E to 145°E using the 925 hPa geopotential height of the NCEP FNL reanalysis data to identify the dominant synoptic patterns over the Korean Peninsula during 2015–2019 (Fig. 1a). Geopotential height is closely associated with various meteorological variables such as temperature, relative humidity, and wind speed (Okoro et al., 2018; Nassif et al., 2020). The clustering results using multivariate input data, including sea-level pressure and temperature anomalies, showed patterns similar to those obtained with univariate input data (Shin et al., 2022). Therefore, this study used geopotential height for the K-means clustering analysis. K-means clustering analysis, a commonly used nonhierarchical method, forms a cluster by classifying data into clusters closest to the center by calculating the distance between the mean value (center value) of each group and individual data. This method is suitable for continuous data processing by rearranging the similarity of data, fast computation, and the easy discovery of clusters in large amounts of data (Lee et al., 2020; Yoon et al., 2018). In general, K-means clustering analysis is implemented as follows: 1) determine the number of clusters k; 2) set k initial centroids arbitrarily; 3) assign each data point to the cluster with the nearest centroid; 4) calculate the average of the classified cluster data to determine the new centroids of the k clusters; and 5) repeat steps 3 and 4 until there is no change in the clusters (Govender and Sivakumar, 2020). In this study, we used the explained cluster variance (ECV) to select the optimal number of clusters (k). The ECV is based on the ratio of the within-group sum of squares (WSS) to the total sum of squares (TSS) for each cluster, as given by Eq. (1) (Cho et al., 2019; Makles, 2012; Ning et al., 2019).

$$ECV = 1 - \frac{WSS}{TSS}, \tag{1}$$

WSS represents the sum of the squared distances between the cluster centroids and the corresponding data, and TSS is the sum of the squared distances between all elements and the centroid of the entire dataset, which is the value of WSS when the cluster number k is one, as shown in Eq. (2).

$$WSS = \sum_{k=1}^{n} \sum_{i=1}^{m} (x_{ik} - \bar{x}_k)^2, \tag{2}$$

Table 1
The frequency of occurrence, averaged $PM_{2.5}$ concentration and the occurrence ratio of five clusters according to $PM_{2.5}$ concentration criteria on each cluster.

Cluster	Frequency	$PM_{2.5}$_AVG	$PM_{2.5}$_Levels			
			G	M	P	V
C1	163 (27.7%)	34.1 μg m^{-3}	21.5%	41.1%	23.3%	14.1%
C2	131 (22.3%)	36.6 μg m^{-3}	9.9%	46.6%	26.7%	16.8%
C3	120 (20.4%)	27.8 μg m^{-3}	30.0%	50.0%	13.3%	6.7%
C4	109 (18.5%)	20.0 μg m^{-3}	70.6%	22.0%	7.3%	0%
C5	65 (11.1%)	36.7 μg m^{-3}	7.7%	53.8%	24.6%	13.8%

x_{ik} is the data corresponding to k clusters, $\bar{x}_k$ is the mean value of k clusters. After calculating the ECV values, the optimal k value was determined based on the difference between ECV values (Zong et al., 2021).

$$\Delta ECV = ECV_k - ECV_{k-1} \tag{3}$$

The ECV ranges from 0 to 1, gradually increases, and saturates to a value close to 1 as the number of clusters increases. In addition, greater ECV and ΔECV values indicate that the clusters are classified more clearly. Therefore, the optimal number of clusters (k) was determined to be 5 by considering each value (Fig. S1).

2.2.2. Definition of pollution levels

Because air quality standards for fine dust are set by considering the environment and characteristics of fine dust in each country, the air quality standards for $PM_{2.5}$ in the Republic of Korea and the European Union are set differently, as shown in Fig. S2. We referred to the air quality standards of the Republic of Korea and the European Union for the acquisition of research data and distribution of $PM_{2.5}$ concentrations in the Seoul area. Therefore, the $PM_{2.5}$ pollution standards were divided into four levels: good (G) for daily average $PM_{2.5}$ concentration of 20 μg m^{-3} or less, moderate (M) for 21–35 μg m^{-3}, poor (P) for 36–50 μg m^{-3}, and very poor (V) for 51 μg m^{-3} or more (Fig. S2).

2.2.3. $PM_{2.5}$ change rate and index of atmospheric dispersion

The $PM_{2.5}$ daily change rate and the Ventilation Index (VI) were used to identify factors affecting the accumulation and diffusion of air pollutants in each synoptic pattern classified by cluster analysis. The $PM_{2.5}$ daily change rate is a variable that can identify $PM_{2.5}$ accumulation and dissipation rate through the difference between the daily average $PM_{2.5}$ concentration of the current day and the previous day and is calculated using Eq. (4) (Hou et al., 2020).

$$dPM_{2.5}{}^{d} = PM_{2.5}{}^{d} - PM_{2.5}{}^{d-1} \tag{4}$$

$PM_{2.5}{}^{d}$ is the daily average concentration of $PM_{2.5}$ on the day (d), $PM_{2.5}{}^{d-1}$ is the daily average concentration of $PM_{2.5}$ on the previous day (d-1). $dPM_{2.5}{}^{d}$ greater than 0 indicates an increase in $PM_{2.5}$ from the previous day (accumulation); conversely, $dPM_{2.5}{}^{d}$ less than 0 indicates a decrease in $PM_{2.5}$ from the previous day (dissipation).

The VI (Ventilation Intensity) is a parameter that indicates how effectively air pollutants can be transported within the PBL height and can be used to evaluate the extent of air pollutants dispersion. It can be calculated as the product of PBL height and wind speed, as shown in Eq. (5) (Pan et al., 2019).

$$VI = PBLH \times WS \tag{5}$$

VI, PBLH, and WS represent the Ventilation Index (m^2 s^{-1}), daily average PBL height (m), and daily average wind speed (m s^{-1}), respectively. A higher VI indicates that the air pollutants within the PBL can be transported and dispersed more effectively (Kim et al., 2022).

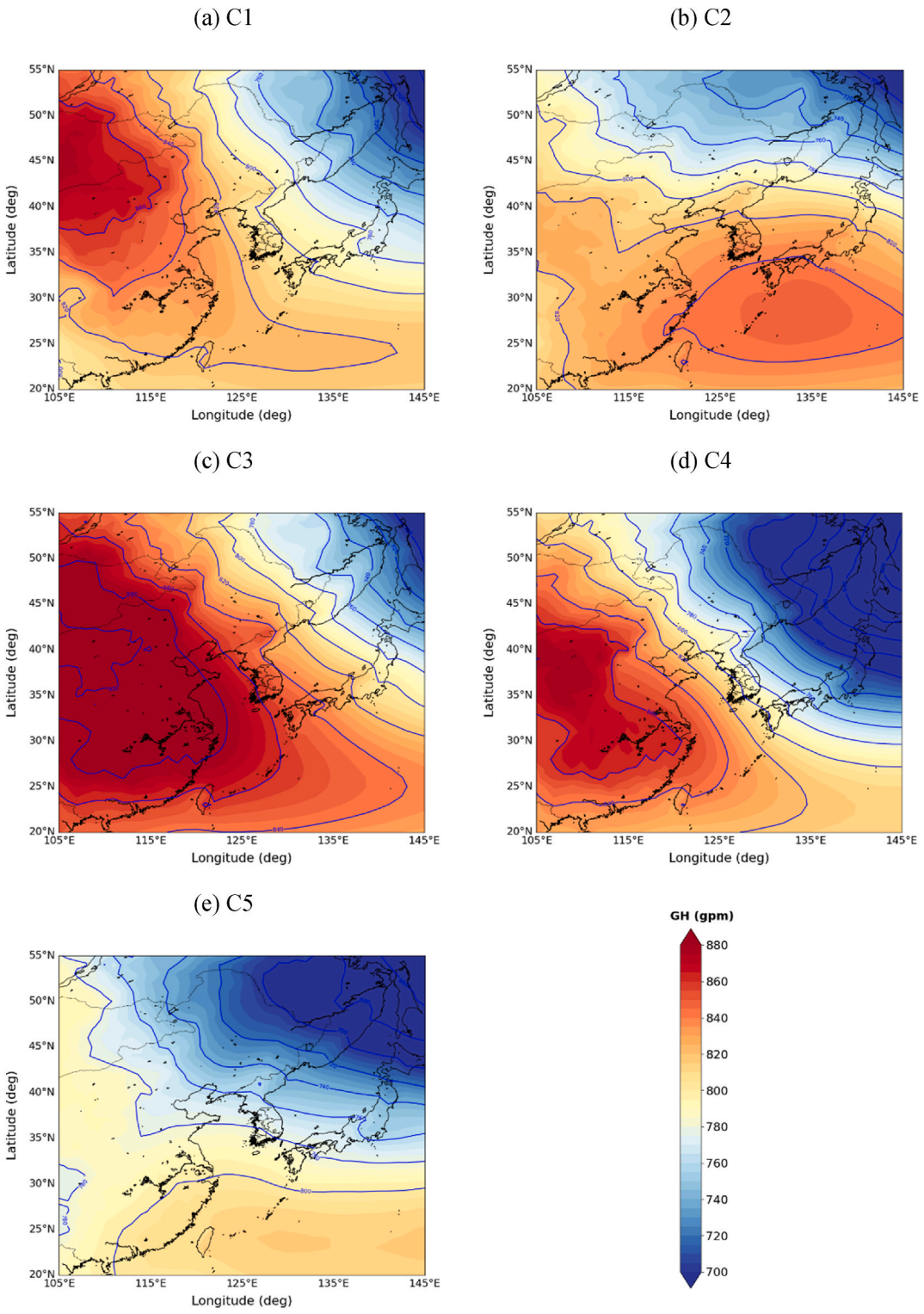

Fig. 2. The five different synoptic patterns of 925 hPa geopotential height in winter from January 2015 to December 2019.

3. Results

3.1. Synoptic patterns analysis and $PM_{2.5}$ distribution

The synoptic patterns occurring on the Korean Peninsula during January, February, March, and December from 2015 to 2019 were divided into five types using K-means clustering analysis. Table 1 shows the frequency of occurrence and mean $PM_{2.5}$ concentration for each cluster, and the occurrence ratio of the five clusters categorized into four different $PM_{2.5}$ pollution levels. That is based on the daily average concentration data of the Seoul area. The clusters were named C1–C5 based on their frequencies of occurrence. Among the five clusters, C1 had the highest frequency at 27.7% of the 588 days, whereas C5 had the lowest frequency at 11.1%. The average concentrations of $PM_{2.5}$, C2, and C5 were 36.6 μg m^{-3} and 36.7 μg m^{-3}, respectively, whereas C4 had the lowest concentration of 20.0 μg m^{-3} among the five clusters. Figs. 2

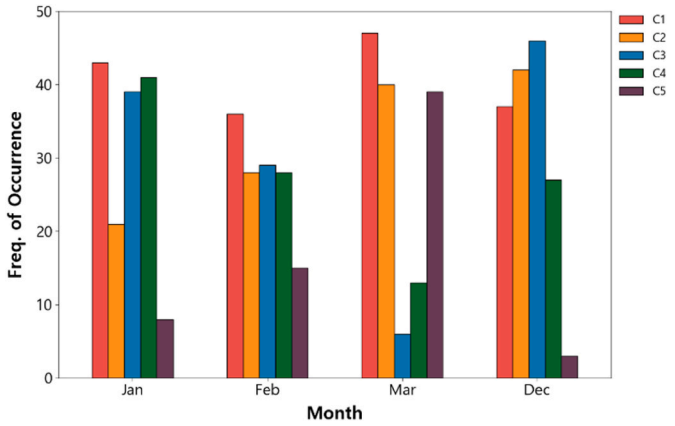

Fig. 3. The frequency of occurrence on each cluster according to four months.

and 3 show the geopotential height at the 925 hPa level for the five clusters and the monthly occurrence frequency of each cluster. During C1, high pressure was observed in the northeastern region of China and weak low pressure was observed over the Kamchatka Peninsula, resulting in a pressure gradient from southwest to northeast. Therefore, northwesterly winds prevailed over the Korean Peninsula. This synoptic pattern was the most frequently occurred on the Korean Peninsula during the study period and average $PM_{2.5}$ concentration was high for 34.1 μg m^{-3}. (Fig. 2a–Table 1). This cluster occurred consistently each month, but was most frequent in March (47 days) (Fig. 3). C2 is a synoptic pattern in which a small-scale independent high pressure is situated southeast of the Korean Peninsula. This pattern influences the occurrence of high $PM_{2.5}$ concentrations in the Seoul area, with a concentration of 36.6 μg m^{-3} (Fig. 2b–Table 1). It occurred frequently in March and December with frequencies of 40 and 42 days, respectively. (Fig. 3). During C3, when strong high pressure was situated in the central region of China, it significantly extended southeastward, affecting the southeastern region of China and the Korean Peninsula (Fig. 2c). In this cluster, strong northwesterly winds occurred owing to the significant pressure gradient from southwest to northeast. The average $PM_{2.5}$ concentration was low at 27.8 μg m^{-3} and this pattern frequently occurred in January and December on 39 and 46 days, respectively (Table 1–Fig. 3). During the C4, high pressure over central China extended southeastward, and a strong low pressure occurred over the Kamchatka Peninsula. Similar to C3, a larger pressure gradient appeared from southwest to northeast (Fig. 2d). In this synoptic pattern, while the intensity of the high pressure located in the central region of China was weaker than that in C3, the intensity of the low pressure situated on the Kamchatka Peninsula was much stronger. Consequently, the pressure gradient in C4 was significantly larger than that in C3, which resulted in strong northwesterly winds. Consequently, the $PM_{2.5}$ concentration was the lowest among the five clusters at 20.0 μg m^{-3}, and it occurred most frequently in January with a frequency of 41 days (Table 1–Fig. 3). C5 is a pattern characterized by large-scale high pressure located to the south of the Japanese mainland and low pressure positioned over the Kamchatka Peninsula (Fig. 2e). At a $PM_{2.5}$ concentration of 36.7 μg m^{-3}, it exhibited the highest concentration among the five clusters, potentially influencing high $PM_{2.5}$ levels in the Seoul area. Although it had the lowest frequency of occurrence, it was the highest in March (Table 1–Fig. 3).

The distribution of mean $PM_{2.5}$ concentrations over the Korean Peninsula when the five classified synoptic patterns occurred is presented in Fig. 4. C1, C2, and C5 generally showed high $PM_{2.5}$ concentrations in the Seoul metropolitan area and Chungcheong-do Province, and the number of poor (very poor) sites was significant in C1, C2, and C5, with 162 (17), 171 (11), and 170 (27) sites, respectively. The C1 showed high concentrations of 50 μg m^{-3} or more in the southern part of Gyeonggi-do Province and Chungcheongbuk-do Province, the C2 exhibited high concentrations in the vicinity of the Seoul metropolitan area, and C5 had high concentrations in the northern part of Chungcheongnam-do Province and the southern part of Gyeonggi-do Province. C3 and C4 generally exhibited low $PM_{2.5}$. The C3 had a total of 263 sites meeting the moderate standard, with $PM_{2.5}$ concentrations ranging from 21 to 35 μg m^{-3}, while the number of good sites was most significant during C4, with 181 sites, and there were no sites for poor and very poor standard.

The synoptic patterns primarily observed on the Korean Peninsula were classified into five clusters: C1, C3, and C4 with a west-to-east pressure distribution and C2 and C5 with a south-to-north pressure distribution. C1, C3, and C4 showed differences in $PM_{2.5}$, depending on the intensity and location of the Siberian High. C4, which had the largest pressure gradient between the Siberian high and low pressures over the Kamchatka Peninsula (C4 > C3 > C1), exhibited the lowest $PM_{2.5}$. C2 and C5, characterized by north-south pressure gradients, showed high $PM_{2.5}$. These patterns may have contributed to the high concentrations in Seoul. C2 was influenced by migratory high pressure in the southern part of the Korean Peninsula, and C5 was affected by the synoptic-scale North Pacific high and Aleutian low.

3.2. *Difference in synoptic patterns according to pollution levels*

Through cluster analysis, the synoptic patterns occurring on the Korean Peninsula during seasonal $PM_{2.5}$ management from 2015 to 2019, were classified into five clusters. We conducted an analysis of the synoptic meteorological differences based on $PM_{2.5}$ pollution levels for each cluster. Overall, except for C4, all clusters had a high proportion within the moderate level, ranging from 40 to 50% (Table 1). In particular, C3 and C5 accounted for a significant proportion (50.0% and 53.8%, respectively). In addition, the proportion of poor and very poor levels was high in C1, C2, and C5, with high average $PM_{2.5}$ concentrations. The proportions of poor and very poor levels were 26.7% and 16.8%, respectively, while the proportion of good levels was 9.9% in cluster C2, which had a higher proportion of poor and very poor levels and a lower proportion of good levels in the $PM_{2.5}$ concentration standard compared to other clusters.

Fig. 5 shows the average daily $PM_{2.5}$ change rates in each cluster. In the synoptic pattern of C1, The accumulation days (83) was higher than the dissipation days (78), but the $PM_{2.5}$ change rate was negative value of −0.9 μg $m^{-3}day^{-1}$. This is because there is no significant difference in the frequency of occurrence between the accumulation days and dissipation days, and $PM_{2.5}$ dissipation rate with an average of −13.1 μg $m^{-3}day^{-1}$ is higher than accumulation rate, and there are outliers in distribution of average $PM_{2.5}$ change rate on dissipation days. Therefore, C1 has meteorological conditions that allow pollutants to dissipate slowly. During C2, the $PM_{2.5}$ change rate was positive at 3.9 μg $m^{-3}day^{-1}$, and the accumulation days (81) were twice as much as the dissipation days (44). Therefore, C2 is a synoptic pattern in which pollutants accumulate. During C3, the $PM_{2.5}$ change rate is 2.3 μg $m^{-3}day^{-1}$, indicating an environment where pollutants tend to accumulate on average. In the C3 synoptic pattern, $PM_{2.5}$ accumulation days (70 days) was more frequent than dissipation days and the $PM_{2.5}$ change rate was 2.3 μg $m^{-3}day^{-1}$ resulting accumulation of $PM_{2.5}$. However, the cluster's mean $PM_{2.5}$ concentration and the occurrence rate of high concentrations were low (poor: 13.3%, very poor: 6.7%). To identify the causes, we analyzed the synoptic conditions of the day preceding the formation of C3 cluster. As a result, the synoptic patterns of clusters C1 and C4 predominantly occurred the day before the occurrence of C3 cluster, and a significant majority of these cases, exceeding 80%, met the meteorological conditions conducive to pollutant dissipation, as defined by the Good and Moderate criteria. In addition, when comparing the PBL height and ventilation index of C3 with the cluster with the average $PM_{2.5}$ concentration was high, it was evident that these values were significantly higher. Therefore, it can be concluded that the synoptic pattern for C3 typically exhibited an environment conducive to

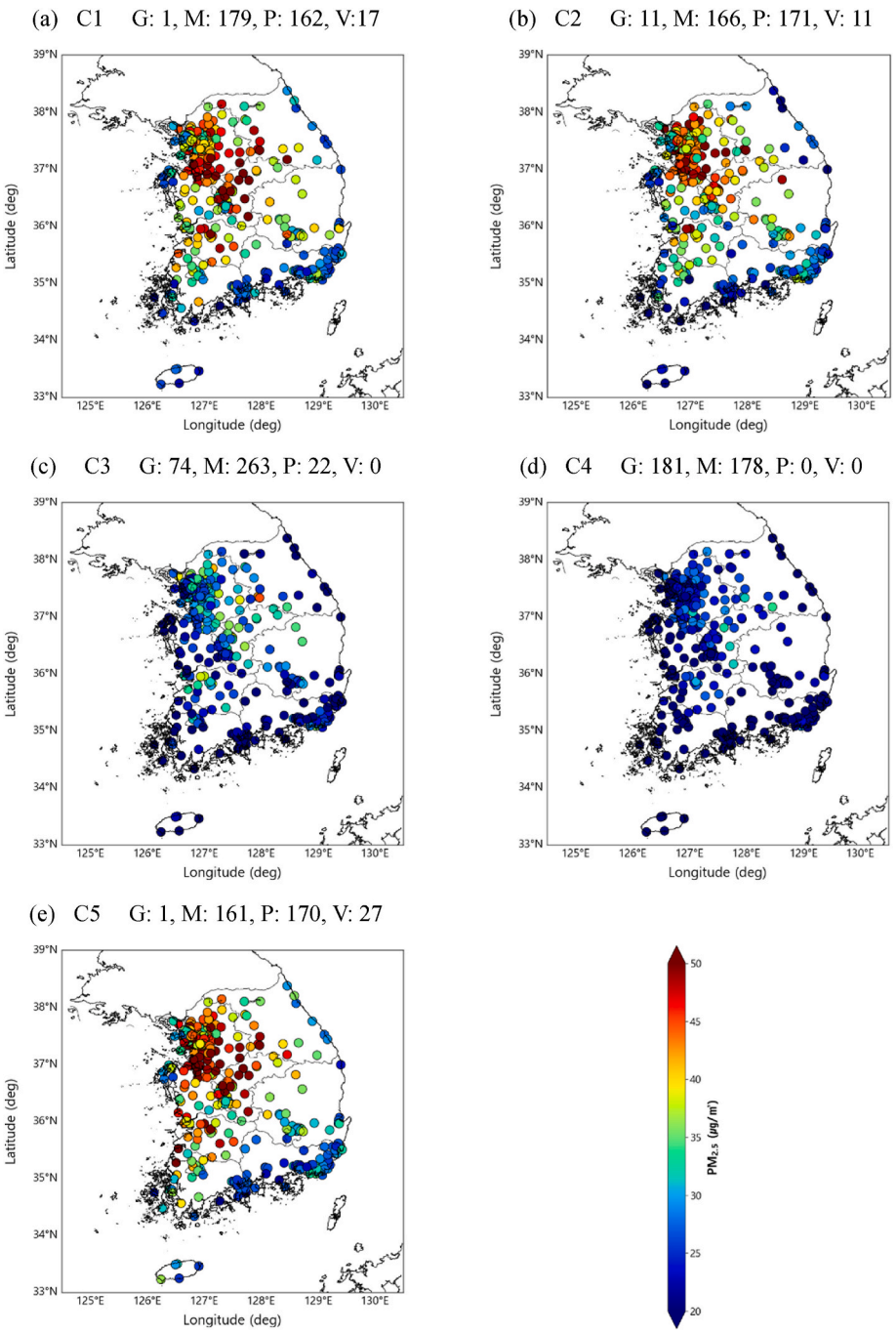

Fig. 4. Mean $PM_{2.5}$ concentration of AQMS in South Korea on each cluster. The numbers in the upper right indicate the number of sites at different pollution levels (G: good, M: moderate, P: poor, V: Very poor).

pollutant accumulation, but the meteorological conditions of the previous day were favorable for significant $PM_{2.5}$ dissipation. Consequently, fewer pollutants accumulated, and the $PM_{2.5}$ concentration was low. In the synoptic pattern of C4, the $PM_{2.5}$ change rate is −6.1 μg $m^{-3}day^{-1}$, indicating a significantly larger negative value compared to other clusters. The number of dissipation days was approximately twice that of accumulation days. Therefore, C4 had meteorological conditions conducive to the dissipation of pollutants. During C5, the $PM_{2.5}$ change rate has a small positive value of 0.5 μg $m^{-3}day^{-1}$. There were more accumulation days (38) than dissipation days (24), but the $PM_{2.5}$ change rate had a small positive value because the distribution of the change rate on the accumulation days was mainly low. Therefore, the C5 meteorological conditions are conducive to slow pollutant accumulation. Overall, clusters with pollutant accumulation ($dPM_{2.5} > 0$) had a higher mean $PM_{2.5}$, whereas clusters with pollutant dissipation ($dPM_{2.5} < 0$) had a lower mean $PM_{2.5}$.

Fig. 6 and S3 the differences in the 925 hPa geopotential height distribution for each cluster (C1-C5) according to $PM_{2.5}$ concentration levels. Table 2 and S1 show the meteorological data in Seoul based on the difference in $PM_{2.5}$ concentration for each cluster. In the case of C1, when the $PM_{2.5}$ concentration criterion was good, strong northwesterly winds occurred due to a significant pressure gradient from southwest to northeast (Fig. 6). Air pollutants transported to the Korean Peninsula from the outside by northerly winds could not accumulate because of the strong wind speed (2.6 m s^{-1}), high PBL height (539.7 m), and ventilation index (1537.3 m^2 s^{-1}) in Seoul and could be transported to other

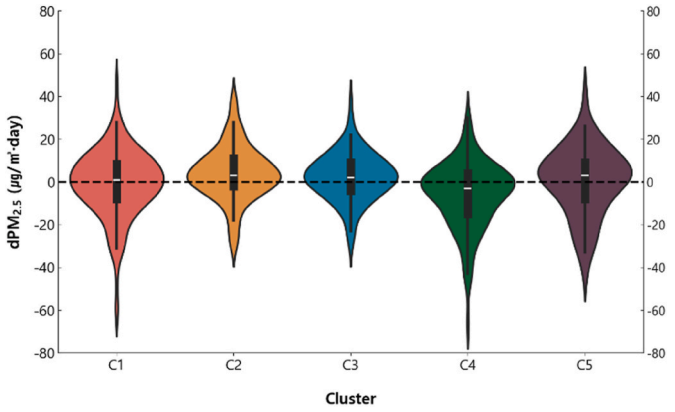

Fig. 5. The average daily $PM_{2.5}$ change rate for the five types of meteorological conditions in Seoul.

regions (Table 2). Under the Poor and Very Poor criteria, the central pressure of the high-pressure system decreased, while that of the low-pressure system increased, resulting in a weakened pressure gradient from southwest to northeast (Fig. 6c and d). This contributed to a reduction in northwesterly winds over the Korean Peninsula. Although the wind speed in Seoul did not exhibit significant changes, the PBL height and ventilation index of 388.2 m and 842.9 $m^2 s^{-1}$, respectively, were significantly lower than those of Good and Moderate, which is conducive to the accumulation of atmospheric pollutants transported from outside.

During C2, the average wind speed (1.9 m s^{-1}) and PBL height (294.4 m) were lower than those of the other clusters in the Seoul area because of the influence of high pressure in the southeastern part of the Korean Peninsula, resulting in the accumulation of air pollutants (Table 2-Fig. 2b). Under the Moderate condition, positive anomalies in geopotential height were observed around the Korean Peninsula, indicating an expansion of the high-pressure system over the region (Fig. 6f). As $PM_{2.5}$ concentrations increased to the Poor level, the positive geopotential height anomalies became more widespread across the Korean Peninsula and surrounding regions (Fig. 6g). Under the Very Poor condition, the high-pressure center shifted toward the southern part of the Korean Peninsula and intensified further (Fig. 6h). As air quality deteriorated, the high-pressure system expanded and migrated closer to the Korean Peninsula. Consequently, the wind direction in the western part of the Korean Peninsula changed from southwesterly to westerly, accompanied by a weakening of the north–south pressure gradient and a subsequent decrease in wind speed. Also, the temperature (3.8 °C → 4.9 °C) and relative humidity (56.8 % → 63.4 %) increased, and the wind speed (2.3 m s^{-1} → 1.6 m s^{-1}) and PBL height (420.6 m → 303.3 m) decreased in the Seoul. These meteorological conditions contribute to high air pollutant concentrations (Table 2). $PM_{2.5}$ accumulated ($dPM_{2.5} > 0$) in all air quality standards except for Good. Therefore, it can be concluded that the C2 synoptic pattern shows high $PM_{2.5}$, due to the transportation and local accumulation of air pollutants caused by weak westerly winds.

During C3, when the $PM_{2.5}$ concentration criterion was good, strong northwesterly winds occurred owing to the pressure gradient from southwest to northeast caused by the strong high pressure located in the central part of China and the low pressure over the Kamchatka Peninsula (Fig. S3). Due to the strong northwesterly winds, atmospheric pollutants can be efficiently dissipated ($dPM_{2.5}$: −4.7 μg $m^{-3}day^{-1}$) (Table S1). During the transition from Moderate to Very Poor levels, both the high-pressure system over central part of China and the low-pressure system over the Kamchatka Peninsula exhibited a weakening trend (Fig. S3 b-d). Consequently, the pressure gradient from southwest to northeast decreased, causing a reduction in wind speeds and an environment conducive to pollutant accumulation ($dPM_{2.5} > 0$).

During C4, where high pressure was located in central China and low pressure was located in the Kamchatka Peninsula, an average wind speed, PBL height and ventilation index were higher with 2.7 m s^{-1}, 645.8 m, and 1924.7 $m^2 s^{-1}$ in the Seoul area compared to other clusters, which promotes the dissipation of pollutants (Table S1). As the $PM_{2.5}$ concentration standard shifts from Moderate to Poor, the central pressure of the high-pressure system over central China decreased, while that of the low-pressure system over the Kamchatka Peninsula increased. As a result, the pressure gradient in the southwest–northeast direction was weakened (Fig. S3f and S3g). Nevertheless, strong northwesterly winds persisted across the Korean Peninsula, and the Seoul area continued to experience high wind speeds. The C4 synoptic pattern was classified as good, with more than 70% of the total number of occurrences; poor, with a very low frequency of 7.3%; and very poor, with no occurrences. In addition, the overall wind speed, PBL height, and ventilation index were significant, suggesting that these clusters may influence low $PM_{2.5}$ in the Seoul area.

In the case of C5, when the $PM_{2.5}$ concentration criterion is good, a large-scale high-pressure system is located to the south of the Japanese mainland, and a strong low-pressure system is located over the Kamchatka Peninsula (Fig. 6i). This results in a pressure gradient from southwest to northeast, leading to northwesterly winds over the Korean Peninsula. The wind speed was high at 2.8 m s^{-1} and $PM_{2.5}$ was in a dissipative state ($dPM_{2.5} < 0$) (Table 2). Under the Moderate condition, negative geopotential height anomalies were observed over eastern China, while positive anomalies appeared near the Kamchatka Peninsula (Fig. 6j). This indicates that the influence of the high-pressure system located south of the Japanese mainland has weakened, and the low-pressure system over the Kamchatka region has also diminished in

Table 2
Meteorological parameters on C1, C2 and C5 in Seoul for different pollution levels.

cluster		$PM_{2.5}$ (μg m^{-3})	$dPM_{2.5}$ (μg $m^{-3}day^{-1}$)	T (°C)	WS (m s^{-1})	RH (%)	PBLH (m)	VI ($m^2 s^{-1}$)
C1	Mean	34.1	−0.9	2.2	2.3	54.4	494.2	1312.8
	G	15.3	−4.7	0.4	2.6	49.0	539.7	1537.3
	M	26.9	−3.4	1.0	2.4	54.9	524.8	1453.0
	P	42.1	1.4	4.6	2.3	55.3	462.4	1143.4
	V	70.8	8.3	4.6	2.0	59.5	388.2	842.9
C2	Mean	36.6	3.9	4.6	1.9	57.4	294.4	573.5
	G	15.6	−4.5	3.8	2.3	56.8	420.6	974.7
	M	27.8	0.6	4.4	2.0	55.5	263.7	518.8
	P	41.7	4.9	4.8	1.7	57.3	295.3	544.5
	V	65.4	16.4	4.9	1.6	63.4	303.3	531.8
C5	Mean	36.7	0.4	5.3	2.1	53.7	435.2	990.3
	G	15.2	−15.2	1.8	2.8	37.9	593.0	1757.0
	M	27.6	−0.2	4.4	2.1	53.5	424.2	950.0
	P	41.9	1.9	6.7	2.2	57.5	412.3	943.1
	V	74.4	8.6	8.3	1.8	56.2	431.0	804.8

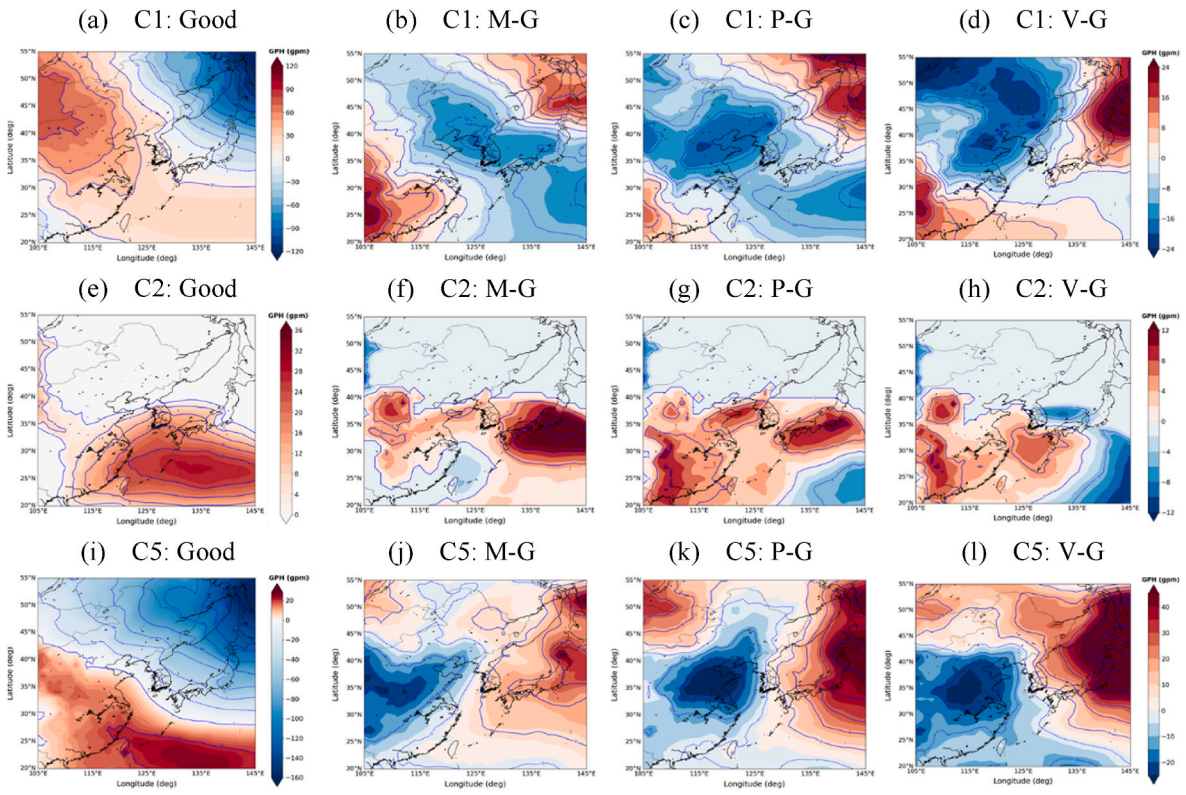

Fig. 6. Differences in the 925 hPa geopotential height (GPH) for clusters C1, C2, and C5 under different $PM_{2.5}$ concentration levels. Panels (a), (e), and (i) show the deviations of the mean GPH under the "Good" (G) $PM_{2.5}$ condition from the overall mean GPH within each respective cluster. Panels (b–d), (f–h), and (j–l) present the differences between the GPH distributions under the "Moderate" (M), "Poor" (P), and "Very Poor" (V) conditions and those under the "Good" condition, respectively, for each cluster.

intensity. As the $PM_{2.5}$ concentration standard deteriorated to Very Poor levels, the negative geopotential height anomalies over eastern China and the positive anomalies near the Kamchatka Peninsula became more pronounced (Fig. 6l). In addition, the appearance of negative anomalies in the high-pressure zone south of Japan suggests an eastward retreat and weakening of the dominant high-pressure system previously situated south of the Korean Peninsula. In parallel, the weakening of the low-pressure system near the Kamchatka Peninsula contributed to a diminished pressure gradient, thereby reducing wind speed across the region. The wind speed was 1.8 m s^{-1}, and the PBL height and ventilation index were 431.0 m and 804.8 m^2 s^{-1}, respectively, under the Very poor standard. Compared with the good standard, there was a decrease in the wind speed and PBL height. The $PM_{2.5}$ change rate was positive value at 8.6 μg $m^{-3}day^{-1}$. These conditions lead to the accumulation of atmospheric pollutants.

During C1, C3, and C4, the $PM_{2.5}$ concentration in Seoul was influenced by changes in the pressure gradient based on the strength of the high- and low-pressure systems located near China and the Kamchatka Peninsula, respectively. During C2, the conditions for the accumulation and dissipation of $PM_{2.5}$, depend on the location and strength of a small-scale high-pressure system located southeast of the Korean Peninsula. In the case of the C5, high and low $PM_{2.5}$ occurred in Seoul, depended on the strength and location of a large-scale high-pressure system located south of the Japanese mainland and a low-pressure system located over the Kamchatka Peninsula.

3.3. *Schematic diagrams of synoptic patterns on Low-$PM_{2.5}$ episodes and High-$PM_{2.5}$ episodes*

Analysis of the synoptic characteristics of each cluster according to $PM_{2.5}$ pollution levels showed that variations in $PM_{2.5}$ concentrations were caused by differences in mesoscale weather conditions within similar synoptic meteorological conditions. Fig. 7 presents schematic diagrams of the synoptic patterns affecting low and high $PM_{2.5}$ episodes in the Seoul by cluster. The main synoptic patterns leading to low $PM_{2.5}$ concentrations in Seoul involve high- and low-pressure systems near China and the Kamchatka Peninsula, respectively. Strong northwesterly winds were induced because of the significant pressure gradient between these two pressure systems (C1 with high pressure located in northeastern China, C3 cluster with strong high pressure in central China, and C4 with strong low pressure over the Kamchatka Peninsula in Fig. 7). Strong northwesterly winds dissipate pollutants transported to the Korean Peninsula from outside, causing low $PM_{2.5}$ concentrations not only in Seoul but throughout the Korean Peninsula. The main synoptic patterns affecting high $PM_{2.5}$ concentrations include C1, which is characterized by weak northwesterly winds due to a decrease in the pressure gradient resulting from the weakening of high pressure in northeastern China and low pressure in the Kamchatka Peninsula; C2, which is characterized by weak westerly winds due to the influence of an isolated high-pressure system located south of the Korean Peninsula; and C5, which is characterized by weak westerly winds as a large-scale high pressure located in the southeast of the Korean Peninsula and low pressure over the Kamchatka Peninsula that weaken and retreat eastward. Weak northwesterly and westerly winds accumulate pollutants transported from the outside, causing high $PM_{2.5}$ concentrations in the Seoul.

4. Conclusions

To analyze variations in $PM_{2.5}$ concentrations in similar synoptic patterns on the Korean Peninsula during seasonal $PM_{2.5}$ management from 2015 to 2019, K-means clustering analysis was performed. In addition, meteorological characteristics for each cluster based on $PM_{2.5}$ concentration standards in Seoul were analyzed using the $PM_{2.5}$ change

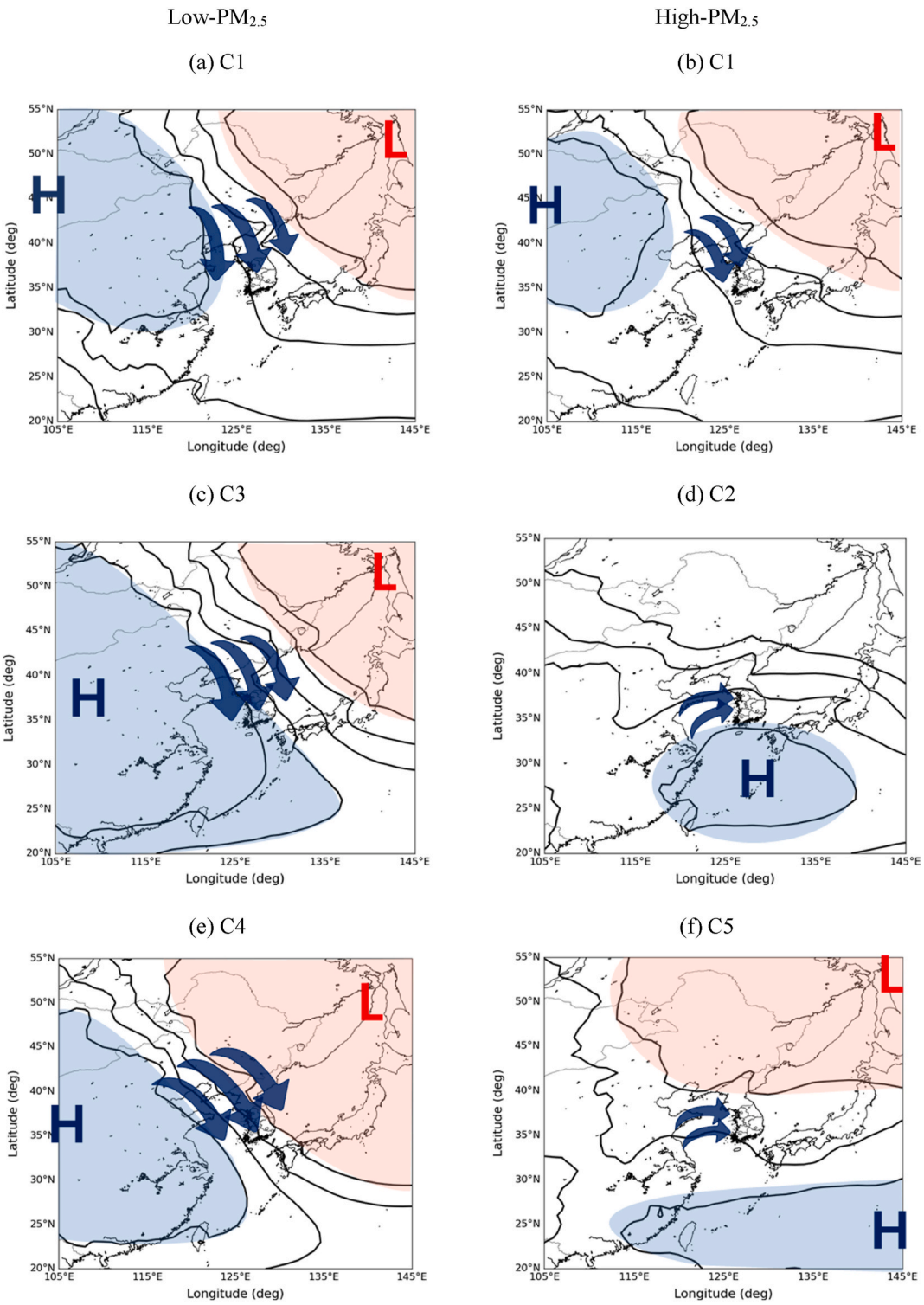

Fig. 7. Schematic diagrams for synoptic patterns leading to low and high $PM_{2.5}$ concentration in Seoul. The black lines represent isopleths of the 925 hPa geopotential height. Color shading indicates regions of high and low pressure, while "H" and "L" indicate the locations of the highest and lowest pressure points within the domain, respectively. (For interpretation of the references to colour in this figure legend, the reader is referred to the Web version of this article.)

rate, and meteorological data (geopotential height, wind speed, PBL height, etc.).

The synoptic patterns were classified into five clusters (C1-C5). The C1, C3, and C4 clusters were characterized by northwesterly winds as the pressure gradient was from southwest to northeast, but there were differences in $PM_{2.5}$ concentrations in the Seoul area depending on the intensity and location of high- and low-pressure systems. The variation in the intensity of the northwesterly winds is a result of the significant pressure gradients between three clusters: a high-pressure system in the northeastern (C1) or central regions of China (C3, C4) and a low-pressure system over the Kamchatka Peninsula, with pressure gradients ranked in the order of C4, C3, and C1. Accordingly, in C4, with the highest pressure gradient, the average $PM_{2.5}$ concentration in Seoul was the lowest at 20.0 μg m^{-3} among the three clusters, while in C1, with the

lowest pressure gradient, the average $PM_{2.5}$ concentration was the highest at 34.1 μg m^{-3} among the three clusters. In the C2 and C5 clusters, westerly winds prevailed as the pressure gradient moved from south to north. The average $PM_{2.5}$ concentrations in Seoul were relatively high at 36.6 μg m^{-3} and 36.7 μg m^{-3}, respectively. The C2 cluster is influenced by a small-scale isolated high pressure located southeast of the Korean Peninsula, whereas C5 cluster is significantly affected by a synoptic-scale North Pacific high pressure located south of the Japanese mainland and an Aleutian low-pressure system northeast of the Korean Peninsula.

We examined the differences in $PM_{2.5}$, within a similar classification cluster, by analyzing the synoptic and meteorological characteristics according to the $PM_{2.5}$ concentration standards for each cluster. During C1, the weakening of the pressure gradient between the high pressure in northeastern China and the low pressure over the Kamchatka Peninsula led to a decrease in the strength of the northwesterly winds, resulting in the deterioration of the $PM_{2.5}$ concentration standard in Seoul. During C2, a small-scale isolated high-pressure system located southeast of the Korean Peninsula moved westward and intensified, resulting in high $PM_{2.5}$ concentrations in the Seoul. During C3 and C4, while there were differences in the strength of the high-pressure system in central China and the low-pressure system in the Kamchatka Peninsula, the weakening of the pressure gradient between them resulted in a deterioration of $PM_{2.5}$ concentration standards in the Seoul area. During C5, the North Pacific high-pressure system located south of the Japanese mainland moved eastward and weakened. The intensity of the Aleutian low-pressure system has also weakened. Consequently, the south-to-north pressure gradient decreased, causing a change in wind direction from northwest to west and a reduction in wind speed. This leads to high $PM_{2.5}$ concentrations in the Seoul.

Based on the results, we summarized the major synoptic patterns that influenced low and high $PM_{2.5}$ episodes in Seoul during the seasonal $PM_{2.5}$ management from 2015 to 2019. Although there are differences in the position and strength of the Siberian high-pressure system, the strong pressure gradient between the Siberian high-pressure system and the low-pressure system over the Kamchatka Peninsula results in strong northwesterly winds that disperse atmospheric pollutants. This leads to a low $PM_{2.5}$ concentrations in Seoul. The decrease in the pressure gradient from southwest to northeast due to the weakening of the Siberian high pressure system (C1), a strong high-pressure system to south of the Korean Peninsula (C2), and a decrease in the south-to-north pressure gradient due to the eastward movement and weakening of the North Pacific high pressure system (C5) caused weak northwesterly and westerly winds, which was conducive to the accumulation of air pollutants and led to high $PM_{2.5}$. This study confirms that air quality can vary depending on the location and strength of high- and low-pressure systems under similar synoptic meteorological conditions.

CRediT authorship contribution statement

Daeun Chae: Writing – original draft, Visualization, Validation, Software, Resources, Methodology, Investigation, Conceptualization. **Jung-Woo Yoo:** Software, Data curation. **Jiseon Kim:** Visualization, Software. **Soon-Hwan Lee:** Writing – review & editing, Validation, Supervision, Funding acquisition, Formal analysis, Conceptualization.

Declaration of competing interest

The authors declare the following financial interests/personal relationships which may be considered as potential competing interests: SOON-HWAN LEE reports financial support was provided by Basic Science Research Program through the National Research Foundation of Korea (NRF). SOON-HWAN LEE reports financial support was provided by the Ministry of Education. If there are other authors, they declare that they have no known competing financial interests or personal relationships that could have appeared to influence the work reported in this paper.

Acknowledgements

This research was supported by the Basic Science Research Program through the National Research Foundation of Korea (NRF), funded by the Ministry of Education (NRF-2020R1A6A1A03044834) and the Korean Government (MSIT) (No. 2022R1A2C1093229).

Appendix A. Supplementary data

Supplementary data to this article can be found online at https://doi.org/10.1016/j.atmosenv.2025.121288.

Data availability

Data will be made available on request.

References

Cho, Y.-J., Lee, H.-C., Lim, B., Kim, S.-B., 2019. Classification of weather patterns in the East Asia region using the K-means clustering analysis. Atmosphere 29 (4), 451–461. https://doi.org/10.14191/Atmos.2019.29.4.451.

Eck, T.F., Holben, B.N., Kim, J., Beyersdorf, A.J., Choi, M., Lee, S., Koo, J.-H., Giles, D.M., Schafer, J.S., Sinyuk, A., Peterson, D.A., Reid, J.S., Arola, A., Slutsker, I., Smirnov, A., Sorokin, M., Kraft, J., Crawford, J.H., Anderson, B.E., Thornhill, K.L., Diskin, G., Kim, S.-W., Park, S., 2020. Influence of cloud, fog, and high relative humidity during pollution transport events in South Korea: aerosol properties and $PM_{2.5}$ variability. Atmos. Environ. 232, 117530. https://doi.org/10.1016/j.atmosenv.2020.117530.

Gong, S., Liu, Y., He, J., Zhang, L., Lu, S., Zhang, X., 2022. Multi-scale analysis of the impacts of meteorology and emissions on $PM_{2.5}$ and O_3 trends at various regions in China from 2013 to 2020 1: Synoptic circulation patterns and pollution. Sci. Total Environ. 815, 152770. https://doi.org/10.1016/j.scitotenv.2021.152770.

Govender, P., Sivakumar, V., 2020. Application of k-means and hierarchical clustering techniques for analysis of air pollution: a review (1980–2019). Atmos. Pollut. Res. 11 (1), 40–56. https://doi.org/10.1016/j.apr.2019.09.009.

Han, S., Park, Y., Noh, N., Kim, J.-H., Kim, J.-J., Kim, B.-M., Choi, W., 2023. Spatiotemporal variability of the $PM_{2.5}$ distribution and weather anomalies during severe pollution events: observations from 462 air quality monitoring stations across South Korea. Atmos. Pollut. Res. 14 (3), 101676. https://doi.org/10.1016/j.apr.2023.101676.

Hou, X., Zhu, B., Kumar, K.R., de Leeuw, G., Lu, W., Huang, Q., Zhu, X., 2020. Establishment of conceptual schemas of surface synoptic meteorological situations affecting fine particulate pollution Across Eastern China in the winter. J. Geophys. Res. Atmos. 125 (23), e2020JD033153. https://doi.org/10.1029/2020JD033153.

Hsu, C.-H., Cheng, F.-Y., 2016. Classification of weather patterns to study the influence of meteorological characteristics on $PM_{2.5}$ concentrations in Yunlin County, Taiwan. Atmos. Environ. 144, 397–408. https://doi.org/10.1016/j.atmosenv.2016.09.001.

Jeong, Y.-C., Yeh, S.-W., Jeong, J.I., Park, R.J., Yoo, C., Yoon, J.-H., 2023. Intrinsic atmospheric circulation patterns associated with high $PM_{2.5}$ concentration days in South Korea during the cold season. Sci. Total Environ. 863, 160878. https://doi.org/10.1016/j.scitotenv.2022.160878.

Kim, Y.-U., Do, H.-S., Kim, J.-H., Kwak, K.-H., Ahn, J., Kim, H., 2022. Applicability study of atmospheric circulation and ventilation indices to analysis of $PM_{2.5}$ episode in March 2018. J. Korean Soc. Atmos. Environ. 38 (4), 542–556. https://doi.org/10.5572/KOSAE.2022.38.4.542.

Ku, H.-Y., Noh, N., Jeong, J.-H., Koo, J.-H., Choi, W., Kim, B.-M., Lee, D., Ban, S.-J., 2021. Classification of large-scale circulation patterns and their spatio-temporal variability during High-PM_{10} events over the Korean Peninsula. Atmos. Environ. 262, 118632. https://doi.org/10.1016/j.atmosenv.2021.118632.

Lee, D., Kim, H.C., Jeong, J.-H., Kim, B.-M., Lee, D.G., Choi, J.-Y., Song, M.Y., Yoon, J.-H., 2022. Relationship between synoptic weather pattern and surface particulate matter (PM) concentration during winter and spring seasons over South Korea. J. Geophys. Res. Atmos. 127 (24), e2022JD037517. https://doi.org/10.1029/2022JD037517.

Lee, H.-C., Cho, Y.-J., Lim, B., Kim, S.-B., 2020. Study on the association of casualties and classification of heat wave weather patterns in South Korea using K-means clustering analysis. J. Korean Soc. Hazard Mitig. 20 (3), 11–18. https://doi.org/10.9798/KOSHAM.2020.20.3.11.

Liu, Y., He, J., Lai, X., Zhang, C., Zhang, L., Gong, S., Che, H., 2020. Influence of atmospheric circulation on aerosol and its optical characteristics in the pearl river delta region. Atmosphere 11 (3), 288. https://doi.org/10.3390/atmos11030288.

Lu, S., Gonga, S., Chen, J., He, J., Zhang, L., Mo, J., 2021. Impact of Arctic Oscillation anomalies on winter $PM_{2.5}$ in China via a numerical simulation. Sci. Total Environ. 779, 146390. https://doi.org/10.1016/j.scitotenv.2021.146390.

Makles, A., 2012. Stata tip 110: how to get the optimal k-means cluster solution. STATA J. 12, 347–351. https://doi.org/10.1177/1536867X1201200213.

Mao, F., Zang, L., Wang, Z., Pan, Z., Zhu, B., Gong, W., 2020. Dominant synoptic patterns during wintertime and their impacts on aerosol pollution in Central China. Atmos. Res. 232, 104701. https://doi.org/10.1016/j.atmosres.2019.104701.

Miao, Y., Guo, J., Liu, S., Liu, H., Li, Z., Zhang, W., Zhai, P., 2017. Classification of summertime synoptic patterns in Beijing and their associations with boundary layer structure affecting aerosol pollution. Atmos. Chem. Phys. 17 (4), 3097–3110. https://doi.org/10.5194/acp-17-3097-2017.

Nassif, W.G., Nemah, H.A., Sada, B.A., 2020. Study of geopotential height values and its interaction with temperature degree over Baghdad city. Iraq. Plant Arch. 20 (2), 1388–1391.

Ning, G., Yim, S.H.L., Wang, S., Duan, B., Nie, C., Yang, X., Wang, J., Shang, K., 2019. Synergistic effects of synoptic weather patterns and topography on air quality: a case of the Sichuan Basin of China. Clim. Dyn. 53, 6729–6744. https://doi.org/10.1007/s00382-019-04954-3.

Okoro, U.K., Chen, W., Nath, D., 2018. Recent variations in geopotential height associated with West African monsoon variability. Meteorol. Atmos. Phys. 131, 553–565. https://doi.org/10.1007/s00703-018-0593-6.

Pan, L., Xu, J., Tie, X., Mao, X., Gao, W., Chang, L., 2019. Long-term measurements of planetary boundary layer height and interactions with $PM_{2.5}$ in Shanghai. China. Atmos. Pollut. Res. 10 (3), 989–996. https://doi.org/10.1016/j.apr.2019.01.007.

Shin, Y., Kim, J.-H., Chun, H.-Y., Jang, W., Son, S.W., 2022. Classification of synoptic patterns with mesoscale mechanisms for downslope windstorms in Korea using a self-organizing map. J. Geophys. Res. 127 (6), e2021JD035867. https://doi.org/10.1029/2021JD035867.

Wang, X., Zhang, R., 2020. Effects of atmospheric circulations on the interannual variation in $PM_{2.5}$ concentrations over the Beijing–Tianjin–Hebei region in 2013–2018. Atmos. Chem. Phys. 20 (13), 7667–7682. https://doi.org/10.5194/acp-20-7667-2020.

Yoon, D., Cha, D.-H., Lee, G., Park, C., Lee, M.-I., Min, K.-H., 2018. Impacts of synoptic and local factors on heat wave events over southeastern region of Korea in 2015. J. Geophys. Res. 123 (21), 12081–12096. https://doi.org/10.1029/2018JD029247.

Zong, L., Yang, Y., Gao, M., Wang, H., Wang, P., Zhang, H., Wang, L., Ning, G., Liu, C., Li, Y., Gao, Z., 2021. Large-scale synoptic drivers of co-occurring summertime ozone and $PM_{2.5}$ pollution in eastern China. Atmos. Chem. Phys. 21 (11), 9105–9124. https://doi.org/10.5194/acp-21-9105-2021.

Zhang, Y., Ding, A., Mao, H., Nie, W., Zhou, D., Liu, L., Huang, X., Fu, C., 2016. Impact of synoptic weather patterns and inter-decadal climate variability on air quality in the North China Plain during 1980-2013. Atmos. Environ. 124, 119–128. https://doi.org/10.1016/j.atmosenv.2015.05.063.

Zhao, S., Feng, T., Tie, X., Long, X., Li, G., Cao, J., Zhou, W., An, Z., 2018. Impact of climate change on Siberian High and wintertime ai r pollution in China in past two decades. Earths Future 6 (2), 118–133. https://doi.org/10.1002/2017EF000682.